



HAL
open science

Discovery of Human-Similar Gene Fusions in Canine Cancers

Ronan Ulvé, Mélanie Rault, Mathieu Bahin, Laetitia Lagoutte, Jérôme Abadie, Clotilde de Brito, Jean-Michel Coindre, Nadine Botherel, Audrey Rousseau, Valentin Wucher, et al.

► **To cite this version:**

Ronan Ulvé, Mélanie Rault, Mathieu Bahin, Laetitia Lagoutte, Jérôme Abadie, et al.. Discovery of Human-Similar Gene Fusions in Canine Cancers. *Cancer Research*, 2017, 77 (21), pp.5721-5727. 10.1158/0008-5472.CAN-16-2691 . hal-01647128

HAL Id: hal-01647128

<https://univ-rennes.hal.science/hal-01647128>

Submitted on 29 Nov 2017

HAL is a multi-disciplinary open access archive for the deposit and dissemination of scientific research documents, whether they are published or not. The documents may come from teaching and research institutions in France or abroad, or from public or private research centers.

L'archive ouverte pluridisciplinaire **HAL**, est destinée au dépôt et à la diffusion de documents scientifiques de niveau recherche, publiés ou non, émanant des établissements d'enseignement et de recherche français ou étrangers, des laboratoires publics ou privés.

Discovery of human-similar gene fusions in canine cancers

Ronan Ulvé^{1,2,3*}, Mélanie Rault^{1,3*}, Mathieu Bahin^{1,3}, Laetitia Lagoutte^{1,3}, Jérôme Abadie⁴, Clotilde De Brito^{1,3}, Jean-Michel Coindre⁵, Nadine Botherel^{1,3}, Audrey Rousseau⁶, Valentin Wucher^{1,3}, Edouard Cadieu^{1,3}, Catherine Thieblemont⁷, Christophe Hitte^{1,3}, Laurence Cornevin⁸, Florian Cabillic⁸, Laura Bachelot^{1,3}, David Gilot^{1,3}, Benoit Hennuy⁹, Thierry Guillaudeau^{3,10}, Arnaud Le Goff^{2,3}, Thomas Derrien^{1,3}, Benoît Hédan^{1,3#} and Catherine André^{1,3#}

1 Univ. Rennes 1, CNRS, Institut de Génétique et de Développement de Rennes (IGDR) - UMR6290, 35000 Rennes, FRANCE.

2 BIOTRIAL Pharmacology, Unité de pharmacologie préclinique, 7-9 rue Jean-Louis Bertrand, 35043 Rennes, FRANCE.

3 UMS 3480 CNRS/US018 INSERM Biosit, Laboratoire commun Oncotrial, 2 Avenue du Pr Leon Bernard, 35043 Rennes, FRANCE.

4 ONIRIS, AMaROC, Ecole Nationale Vétérinaire, Agroalimentaire et de l'Alimentation Nantes Atlantique, 44307 Nantes, FRANCE.

5 Institut Bergonié, 229, cours de l'Argonne, 33076 Bordeaux, FRANCE.

6 Département de Pathologie Cellulaire et Tissulaire, CHU, 4 rue Larrey, 49100 Angers, FRANCE.

7 APHP, Hopital Saint-Louis, Hemato-oncologie; Université Paris Diderot, Sorbonne Paris Cité, Paris-75010, FRANCE.

8 Laboratoire de cytogénétique et biologie cellulaire, CHU de Rennes, INSERM, INRA, Univ. Rennes 1, Nutrition Metabolisms and Cancer, 35043 Rennes, FRANCE.

9 GIGA-Genomics, Université de Liège, CHU, 1 Avenue de l'Hopital, 4000 Liège, BELGIQUE.

10 ER OSS440 INSERM, Avenue de la Bataille Flandres-Dunkerque, 35000 Rennes, FRANCE.

*These authors equally contributed to this work.

These authors jointly supervised this work.

Running title

Dog/human similar fusions in cancers

Keywords

Fusions, spontaneous model, cancer, dog

Additional information

Grant support: For this study, C Andre had been award grants by CNRS, INCa PLBio "Canine rare tumours" funding (N° 2012-103; 2012-2016), Aviesan/INSERM MTS 2012-06, in the framework of Plan Cancer 2009-2013 and by the CRB-Anim infrastructure, ANR-11-INBS-0003, in the framework of the 'Investing for the Future' program (PIA) and T. Guillaudeau has been awarded by the ANR with the LabCom Oncotrial project 2014-2017. Ronan Ulvé, PhD was funded through a CIFRE contract between CNRS and the Biotrial company (2013-2016). Mélanie Rault, PhD was funded through a French "Ministère de la recherche" funding (2013-2016).

Address correspondence and reprint requests to: Catherine André or Benoit Hedan. CNRS UMR 6290, Institut de Génétique et Développement de Rennes, Université de Rennes 1, 2 Avenue du Pr. Leon Bernard, 35043 Rennes, France. Phone : +3323234509, Fax : +33 (0)2 23 23 44 78. E-mails : catherine.andre@univ-rennes1.fr, benoit.hedan@univ-rennes1.fr

The authors declare no potential conflicts of interest.

Abstract

Canine cancers represent a tremendous natural resource due to their incidence and striking similarities to human cancers, sharing similar clinical and pathological features as well as oncogenic events including identical somatic mutations. Considering the importance of gene fusions as driver alterations, we explored their relevance in canine cancers. We focused on three distinct human-comparable canine cancers representing different tissues and embryonic origins. Through RNA-Seq, we discovered similar gene fusions as those found in their human counterparts: *IGK-CCND3* in B-cell lymphoma, *MPB-BRAF* in glioma, and *COL3A1-PDGFB* in dermatofibrosarcoma protuberans-like. We showed not only similar partner genes but also identical breakpoints leading to oncogene overexpression. This study demonstrates similar gene fusion partners and mechanisms in human-dog corresponding tumors and allows for selection of targeted therapies in preclinical and clinical trials with pet dogs prior to human trials, within the framework of personalized medicine.

Introduction

During the last decade, pet dogs have arisen as a relevant but under-used model for cancer genetics and therapies (1). Although extremely useful for cancer research, rodent models show limitations in their ability to fully reproduce the complexity of spontaneously occurring human tumors (2). Since canine tumors address part of these concerns, there is a growing interest in using this “natural cancer resource” in translational cancer research for both human and dog medicine benefit. Inclusion of pet dogs in preclinical and clinical trials should accelerate the screening of new treatments by reducing the time and cost of evaluating efficacy, pharmacokinetics and toxicity (3). These advantages have already justified ongoing trials with pet dogs (4).

To use canine cancers as models for the development of new treatments, it is essential to determine human and canine tumors correspondences. The physiopathology of canine tumors presents strong similarities with human tumors in their biological behavior, histopathological features and response to treatments (2). Moreover, comparative oncology studies show that some canine and human cancers share similar genetic aberrations including chromosomal instability, common cytogenetic aberrations, involvement of identical oncogenes or tumor suppressors, and even identical somatic mutations (5). The identification of such driver genetic alterations, both in dogs and humans, are highly informative for the development of dedicated new targeted therapies such as the development of c-kit inhibitors for canine mast cell disorders (6). Among such driver events, we focused on translocations that generally lead to overexpression of oncogenes. In humans, these recurrent translocations have been described in hematological disorders, sarcomas and carcinomas; most of them are

specific, and even pathognomonic for tumor types and represent precious tools for diagnosis and relevant therapeutic targets (7,8). Although well described in humans, such translocations in dogs have only been explored and identified by fluorescence *in situ* hybridization (FISH) to date, in two canine hematological tumors: a chronic lymphocytic leukemia with a *BCR-ABL* fusion and a Burkitt's lymphoma with a *IGH-MYC* translocation (9).

In the present study, we aim to demonstrate that pet dogs are relevant spontaneous models for human oncology with conserved key gene fusions, not restricted to hematological disorders by identifying chimeric transcripts with new and highly resolutive methods (NGS). Thus, we used whole transcriptome sequencing (RNA-Seq) of cancers with different origins to allow the detection of gene fusions without preconceived candidates. We report here, for the first time, chimeric transcripts in canine cancers reflecting chromosomal translocations that are comparable to human translocations in: a dermatofibrosarcoma protuberans-like (DFSP-like); an oligodendroglioma; and a diffuse large B-cell lymphoma (DLBCL). We then validated these gene fusions on DNA and RNA from the tumors, providing the breakpoint positions at the single-nucleotide resolution. We finally showed that similarly to the orthologous human cancers, these canine cancers not only share identical breakpoints but also overexpression of the targeted oncogenes. These striking molecular similarities between human and canine cancers pave the way for the use of the canine model in targeted therapies for the benefit of both human and dog patients.

Material & Method

Samples

Blood and tissue biopsy samples from dogs were collected by a network of veterinarians through the Cani-DNA biobank (<http://dog-genetics.genouest.org>), which is part of the CRB-Anim infrastructure. The work with dog samples was approved by the CNRS ethical board, France (35-238-13) for UMR6290 and dog owners consented to the use of data for research purposes anonymously. We selected 3 distinct cancers (lymphomas, sarcomas and gliomas) representing different tissues (neurological, subcutis, hematological) and different embryonic origins, with known fusions in the human counterpart. The set of samples included 3 lymphomas (2 DLBCLs and 1 T lymphoma), 2 gliomas and 1 dermatofibrosarcoma protuberans-like.

Histological diagnosis

The diagnosis of the six tumors was re-evaluated by dedicated veterinary (JA) and human pathologists (JMC and AR for the DFSP-like and the glioma respectively). Immunohistochemical staining was performed using antibodies showing reactivity with the dog's protein according to the manufacturer or to biocompare website: anti CD34 (Santa Cruz Biotechnology Dallas, TX, Ref SC-7045) and anti PDGFB (Novus Biological, Littleton, CO, Ref NBP1-52533), anti BRAF (Abbiotec, San Diego, CA, Ref 251460), anti CCND3 (Aviva, San Diego, CA, Ref AVARP03038_P050) for the DFSP-like, the glioma and DLBCL respectively. Appropriate negative controls were performed with normal immune serum of rabbit for CCND3 and BRAF, of goat for PDGFRB.

DNA and RNA isolation

The germline DNA from blood, DNA and RNA from tissues were isolated using respectively the Blood L, Tissue and RNA II NucleoSpin® kits (Macherey-Nagel, Duren, Germany) according to the manufacturer's instructions.

RNA-Seq sample preparation and sequencing

RNA-Seq was performed using the GIGA genomics facility. Briefly, Illumina Truseq RNA Sample Preparation kit V2 was used to prepare libraries from 1 μ g of total RNA with a RNA Integrity Number greater than 7.3 (Agilent Technologies, Santa Clara, CA). Poly-A RNAs were purified with polyT-coated magnetic beads and chemically fragmented to a median size of 200 nucleotides. These were used as a template for first strand synthesis in the presence of random hexamers and second strand synthesis afterwards. Next, double stranded cDNA ends were end-blunted and adenylated at 3'OH extremities before ligation to adaptors containing the indexes. Finally, the adapter-ligated library fragments were enriched by PCR following Illumina's protocol and purified with Ampure XP magnetic beads (Agencourt, Beverly, MA). Final libraries were validated on a Bioanalyser DNA 1000 chip (Agilent Technologies, Santa Clara, CA) and quantified by qPCR with the KAPA library quantification kit (Kapa Biosystems, Wilmington, MA). Sequencing was performed on an Illumina HiSeq 2000 instrument using the PE 2X100 cycles protocol.

Identification of fusion transcripts

Candidate gene fusion transcripts were identified with CRAC and chimCT softwares (<http://cractools.gforge.inria.fr/>) using the CanFam3 canine genome reference. Fusion transcripts were manually filtered by discarding transcripts with less than five reads spanning the fusion junction and three reads encompassing the two fusion transcripts, as well as transcripts involving paralogous genes or pseudogenes, transcripts identified as read-through, transcripts with no Ensembl annotation (Supplementary Table 1).

RT-PCR

Reverse transcription was performed on 1 µg of total RNA from tumor or healthy tissue using the High-capacity cDNA Reverse Transcription kit (Applied Biosystems, Foster City, CA) according to the manufacturer's instructions.

Validation of the fused transcript

PCR amplifications were performed on cDNA samples diluted 1:40 using the Type-it Microsatellite PCR kit (Qiagen, Hilden, Germany) with dedicated primers (Supplementary Table 2). PCR products were sequenced with a 370 ABI sequencer using the BigDye Terminator v3.1 cycle sequencing kit (Applied Biosystems, Foster City, CA). The presence of fusion transcripts was assessed by alignment of sequences on the CanFam 3 reference dog sequence (<https://genome.ucsc.edu/>).

Breakpoint mapping on genomic DNA

PCR amplifications were performed on DNA to validate fusion transcripts. Primers specific for each breakpoint (Supplementary Table 2) were designed on CanFam3 to span the candidate introns flanking the identified exons in the chimeric transcripts. All combinations between forward and reverse primers from translocated chromosomes were tested. The large regions of about 1 kb were amplified from 10 ng/µl diluted DNA samples using the Phusion Hot Start II DNA Polymerase kit (Thermo scientific, Waltham, MA).

Exon expression analysis RT-PCR

qRT-PCR was performed on cDNA samples diluted 1:20 with the SYBR Green PCR master mix on the 7900HT Fast Real-Time PCR System (Applied Biosystems, Foster City,

CA) using standard procedures. Each PCR was carried out in triplicate. Relative amounts of the transcript were determined using the delta-delta Ct method. Canine *HPRT* gene (ENSCAFG00000018870) for the lymphoma and the DFSP-like, and *TBP* gene (ENSCAFG00000004119) for the glioma, were used as housekeeping genes. The mRNA levels in each tumor were calculated as a fold increase compared with at least 6 different healthy tissue mRNA controls: 6 healthy skin samples, 8 healthy cortex samples, 6 healthy lymph nodes for the fibrosarcoma, glioma and lymphoma respectively.

Western Blot

Cellular protein extracts were prepared using a cell lysis buffer containing 20mM Tris-HCl pH 7.5, 150mM NaCl, 1mM EDTA, 1mM EGTA and supplemented with 1mM PMSF, 1X EDTA-free cocktail protease inhibitor (Roche Diagnostic, Meylan, France), 30mM sodium fluoride, 40mM glycerol phosphate, 1mM sodium orthovanadate, 0,5% Triton X-100. Protein concentrations were determined by the BCA protein assay (Sigma-Aldrich, St Louis, MO) using bovine serum albumin as a standard.

Protein samples were denatured for 10min at 95°C, and equal amounts of cell proteins (20 µg) were subjected to 10% SDS-PAGE and transferred onto nitrocellulose membranes (Amersham - GEH life, Arlington Heights, IL). Membranes were probed with suitable antibodies. The primary antibodies were: anti-BRAF (Ref 251460, 1:5000, Abbiotec, San Diego, CA) and anti-β-actin (BA3R, 1:5000, Millipore, Temecula, CA). Horseradish-Peroxidase-conjugated secondary antibodies were purchased from Jackson ImmunoResearch (Suffolk, UK). Signals were detected using the LAS-4000 Imager (Fuji Photo Film, Tokyo, Japan). siRNAs were purchased from IDT DNA (Coralville, IO):

siBRAF1 : 5'- CAUGAAGACCUCACAGUAAAAAUAG-3',

siBRAF2 5'- GACCAAUUUGAGAUGAUAAGCTT-3',

siCTR (NC1) 5'-CGUUAUUCGCGUAUAAUACGCGUAT-3'

Two siRNAs targeting *BRAF* were designed to target two distinct regions of *BRAF* (nucleotides 1717-1740, 1599-1623 respectively for ENSCAFT00000006305) and ordered to IDT DNA. siRNAs were transfected into human melanoma cells 501Mel or into a canine oral melanoma cell line, kindly provided by dr D. Tierny, using Lipofectamine RNAiMAX (Life Technologies, Carlsbad, CA) following the manufacturer's instructions. Three days later, BRAF expression levels were analyzed by western-blotting experiments.

FISH experiments

MBP-BRAF fusion tests were performed on 4 µm sections of formalin-fixed paraffin-embedded tissue blocks using the bacterial artificial chromosome (BAC) clones 42G22-97M23 and 160H02-360E1 (<http://bacpacresources.org/library.php?id=253>). These BAC clones were labeled with green-dUTP (Abbott Molecular, Downers Grove, IL) and Cy3-dCTP (Amersham Biosciences, Buckingham-shire, UK) and hybridized proximal to *MBP* and distal to the *BRAF* breakpoint regions, respectively. Slides were analyzed by an experienced cytogeneticist (FC), using a fluorescence microscope (Axioskop2, Axio Imager Z2, Zeiss, Göttingen, Germany) and Isis imaging software (Metasystems, Altlußheim, Germany). Per case, at least 100 non-overlapping tumor nuclei were examined.

Statistics

All statistical tests were performed with the R software.

Results and discussion

Previous cytogenetic studies have underlined the importance of gene fusions in hematological disorders and sarcoma in humans (8). To investigate gene fusions in canine cancers, we analyzed 6 tumors belonging to 3 distinct cancers, representing different tissues (neurological, subcutis, hematological) and embryonic origins, and for which the human corresponding tumors are known to involve key gene fusions. We performed RNA-Seq, using dedicated softwares followed by classical filters and manual curation to exclude false-positive chimeras, we finally identified 3 gene fusions in 3 of the 6 tumors (Table 1 and Supplementary Table 1).

1-A *COL3A1-PDGFB* fusion in a canine dermatofibrosarcoma protuberans-like

In human dermatofibrosarcoma protuberans (DFSP), the translocation t(17;22) leading to the fusion of the Collagen type 1 alpha 1 (*COL1A1*) and Platelet-derived growth factor B chain (*PDGFB*) genes is considered as pathognomonic of DFSP (10). Thus, we analyzed a canine DFSP-like case (Supplementary Figure 1) and we found a chimeric transcript resulting from the fusion between the Collagen type 3 alpha 1 (*COL3A1*) and the *PDGFB* genes. Since *COL3A1* and *COL1A1* are paralogous genes, we anticipated that this canine translocation is similar to the human one. Indeed, as in humans, the breakpoint in *PDGFB* is localized in intron 1 (Figure 1a), moreover the fusion validation on the cDNA and the genomic DNA of this tumor (Figure 1b-d) shows a conserved reading frame between the first *COL3A1* exons and the exon 2 of *PDGFB*. Similar to the situation in human DFSP (11), we hypothesized that this translocation, placing *PDGFB* under the regulation of the *COL3A1* promoter, induces the overexpression of *PDGFB* in the canine DFSP-like tumor. This is confirmed by the expression levels of exons retained in the

chimeric transcript, which are increased on average 9.6-fold in comparison to healthy tissues (p-value <0.001, one-tailed Wilcoxon test) (Figure 1e). Moreover, PDGFB protein is detectable in the tumor by immunostaining (Supplementary Figure 1). Complementary to this, the alignment of canine and human PDGFB protein sequences (Supplementary Figure 2) shows the conservation of the 2 proteolytic cleavage sites in the canine PDGFB and in the putative chimeric protein resulting from *COL3A1/PDGFB* fusion. Under these conditions, the canine *COL3A1/PDGFB* should produce a chimeric precursor protein, transformed into a mature growth factor after proteolysis and forming an autocrine loop, as for the human *COL1A1/PDGFB* fusion (11). Since the chimeric protein *COL1A1/PDGFB* is targeted by imatinib for human DFSP (7,10), regarding the genetic and biological similarities between human DFSP and canine DFSP-like, we predict similarities in treatment responses. Finally, we propose the *COL3A1* gene as a new candidate partner gene for human DFSP, like the recently discovered *COL1A2* (12).

2-A *MBP-BRAF* fusion in a canine glioma

Human gliomas are a heterogeneous group of tumors of the central nervous system with *BRAF* alterations (somatic mutations or fusions) described almost in all subgroups (13). Therefore we analyzed two canine grade 3 anaplastic oligodendrogliomas (WHO classification) (Supplementary Figure 3). In one of them, we identified a relevant chimeric transcript resulting from the fusion between the *Myelin Basic Protein (MBP)* and the *B-Raf proto-oncogene (BRAF)* genes. Like in human gliomas with breakpoints localized between *BRAF* intron 8 and 10 (14), the breakpoint of *BRAF* in this canine glioma is within intron 7, orthologous to human *BRAF* intron 8 (Figure 2a). This fusion

was validated on the cDNA and the genomic DNA of this tumor (Figure 2b-d). The reading frame is conserved between the first *MBP* exons and the last exons of *BRAF*. Since the *MBP* promoter is strongly active in glioma cells (15), we anticipated that this translocation could also induce *BRAF* overexpression. We confirmed this hypothesis by measuring the expression levels of exons retained in the chimeric transcript; there was an average 12.8-fold increase in comparison to healthy tissues (p-value = 0.0039, one-tailed Wilcoxon test) (Figure 2E). Moreover, BRAF protein is detectable in the tumor by immunostaining and a fused protein is detectable in the tumor sample by western blot (Supplementary Figure 3). Since the alignments of the canine and human BRAF protein sequences showed that the canine chimeric protein has lost its N-terminal auto-inhibitory domain (Supplementary Figure 4), this alteration should induce a constitutive BRAF kinase activity as shown in human cancers (16). In human gliomas, *BRAF* is mainly fused with *KIAA1549* but other partners have been described (14), while most of these fusions are found in astrocytomas, they are also reported in oligodendrogliomas (17). We propose *MBP* as a new candidate partner for *BRAF* fusions in human gliomas. For these human tumors, with limited therapeutic options, *BRAF* alterations offer new therapeutic strategies and clinical trials are ongoing (16). In this context, spontaneous canine glioma with *BRAF* fusions provides a unique model to develop new and more efficient treatments.

3-An *IGK-CCND3* fusion in a canine B-cell lymphoma

In human lymphomas, alterations during the natural recombination process of immunoglobulin genes lead commonly to fusions with oncogenes associated with their overexpression. Thus we analyzed 3 canine lymphomas (two DLBCLs, and one T-cell

lymphoma) and found one aberrant transcript revealing a fusion between the *Immunoglobulin light chain kappa locus (IGK)* with *Cyclin-D3 (CCND3)* in one DLBCL sample (Table 1) (Figure 3a). This fusion was validated on the cDNA and the genomic DNA of this tumor (Figure 3b-d). Such translocations involving *CCND3* and immunoglobulin genes have already been described in human B-cell malignancies including DLBCL, which could explain the overexpression of *CCND3* found in 10% of human DLBCL (18). Thus, we anticipated that the canine translocation also induces the overexpression of *CCND3*. This is supported by the fact that *CCND3* is overexpressed in canine DLBCL (Figure 3e) and the *CCND3* protein is easily detectable by immunohistochemistry in the canine DLBCL (Supplementary Figure 5). While, *IGK-CCND3* fusion was not identified in human lymphomas, overexpression of *CCND3* driven by *IG*-mediated translocations are expected and searched in cases showing break-apart probes for *CCND3*. Moreover fusions involving *IGK* and other cyclins, of which *CCND2*, have already been detected (19). In addition, the overexpression of *CCND3* in human DLBCL is a prognostic factor associated with poor clinical outcome (20). Thus, canine lymphomas with fusions involving cyclin D could be used for clinical trials targeting cyclins.

Conclusion

Our work reveals similar fusions in corresponding cancers between dogs and humans and identifies for the first time chimeric transcripts involving the same fused oncogenes with similar rearrangements leading to malignancy. The identification of these three fused transcripts in three different tumors supports the existence of other fused transcripts in other subtypes of canine cancers, similar to what is found in humans. With

NGS methods, which are revolutionizing the identification of gene fusions without preconceived idea of partner genes, such canine models will benefit the scientific community, allowing development of new targeted therapies. In the context of the “One Health” concept, such results of comparative oncology lead us to anticipate that human and veterinary medicine will benefit from clinical trials that include pet dogs as patients.

Acknowledgments

We thank Olivier Albaric and Frédérique Nguyen (AMaROC research unit, Oniris, Ecole Nationale Vétérinaire de Nantes, France) as well as Caroline Laprie (Histopathology laboratory, Amboise, France), Marie Lagadic (Idexx laboratory, Alfort, France), Frédérique Degorce-Rubiale (LAPVSO, Toulouse, France) who provided anatomopathologic diagnoses. We thank the French veterinarians Anne-Sophie Guillory (IGDR, Rennes, France), Marie-Anne Colle (Oniris, Nantes, France), Valérie Gerard (Les Mages, France), Laurie Anne Dulière-Hyrien (Le Plessis-Belleville, France), Arnaud and Claude Muller (Lomme, France), Laurence Armando (Tavaux, France), Catherine Escriou (VetAgro Sup, Lyon, France) and Patrick Devauchelle (MICEN VET, Creteil, France) for providing us with clinical data and samples, as well as dog owners and breeders. We warmly thank Wouters Coppieters, Anne-Sophie Lequarré and Michel Georges (GIGA-Genomics, Université de Liège, Belgique) for RNA-Seq, and Stéphane Dréano (IGDR, Rennes, France) for Sanger sequencing. We thank Alain Fautrel (histopathology platform H2P2, UMS CNRS/INSERM Biosit, Rennes), who kindly provided paraffin tumor sections for histology and immunohistology. We are grateful to Yann Le Cunff (IGDR, Rennes, France), Sylvie Jaillard (Laboratoire de cytogénétique et biologie cellulaire, Faculty of medicine Rennes, France), Rémy Pedoux (Université de Rennes 1/INSERM, Rennes, France) and Meriam Djemai (Biotrial, Rennes, France) for helpful discussions. We thank Aline Primot (IGDR, Rennes, France) for helpful advices on western blot. Finally, we thank Dominique Tierny (ONCOVET-VETOTECH, Villeneuve d'Ascq, France) who kindly provided us an oral canine melanoma cell line for siRNA and western blot experiments.

References

1. Paoloni M, Khanna C. Translation of new cancer treatments from pet dogs to humans. *Nat Rev Cancer*. 2008;8:147–56.
2. Rowell JL, McCarthy DO, Alvarez CE. Dog models of naturally occurring cancer. *Trends Mol Med*. 2011;17:380–8.
3. Paoloni M, Webb C, Mazcko C, Cherba D, Hendricks W, Lana S, et al. Prospective molecular profiling of canine cancers provides a clinically relevant comparative model for evaluating personalized medicine (PMed) trials. *PloS One*. 2014;9.
4. LeBlanc AK, Breen M, Choyke P, Dewhirst M, Fan TM, Gustafson DL, et al. Perspectives from man's best friend: National Academy of Medicine's Workshop on Comparative Oncology. *Sci Transl Med*. 2016;8:324ps5.
5. Schiffman JD, Breen M. Comparative oncology: what dogs and other species can teach us about humans with cancer. *Philos Trans R Soc Lond B Biol Sci*. 2015;370.
6. Ranieri G, Marech I, Pantaleo M, Piccinno M, Roncetti M, Mutinati M, et al. In vivo model for mastocytosis: A comparative review. *Crit Rev Oncol Hematol*. 2015;93:159–69.
7. Greco A, Roccato E, Miranda C, Cleris L, Formelli F, Pierotti MA. Growth-inhibitory effect of STI571 on cells transformed by the COL1A1/PDGFB rearrangement. *Int J Cancer J Int Cancer*. 2001;92:354–60.
8. Mertens F, Johansson B, Fioretos T, Mitelman F. The emerging complexity of gene fusions in cancer. *Nat Rev Cancer*. 2015;15:371–81.
9. Breen M, Modiano JF. Evolutionarily conserved cytogenetic changes in hematological malignancies of dogs and humans--man and his best friend share more than companionship. *Chromosome Res Int J Mol Supramol Evol Asp Chromosome Biol*. 2008;16:145–54.
10. Dhir M, Crockett DG, Stevens TM, Silberstein PT, Hunter WJ, Foster JM. Neoadjuvant treatment of Dermatofibrosarcoma Protuberans of pancreas with Imatinib: case report and systematic review of literature. *Clin Sarcoma Res*. 2014;4.
11. Simon MP, Pedeutour F, Sirvent N, Grosgeorge J, Minoletti F, Coindre JM, et al. Deregulation of the platelet-derived growth factor B-chain gene via fusion with collagen gene COL1A1 in dermatofibrosarcoma protuberans and giant-cell fibroblastoma. *Nat Genet*. 1997;15:95–8.
12. Nakamura I, Kariya Y, Okada E, Yasuda M, Matori S, Ishikawa O, et al. A Novel Chromosomal Translocation Associated With COL1A2-PDGFB Gene Fusion in Dermatofibrosarcoma Protuberans: PDGF Expression as a New Diagnostic Tool. *JAMA Dermatol*. 2015;151:1330–7.
13. Penman CL, Faulkner C, Lowis SP, Kurian KM. Current Understanding of BRAF Alterations in Diagnosis, Prognosis, and Therapeutic Targeting in Pediatric Low-Grade Gliomas. *Front Oncol*. 2015;5.
14. Forbes SA, Beare D, Gunasekaran P, Leung K, Bindal N, Boutselakis H, et al. COSMIC: exploring the world's knowledge of somatic mutations in human cancer. *Nucleic Acids Res*. 2015;43:D805–11.
15. Miyao Y, Shimizu K, Tamura M, Akita H, Ikeda K, Mabuchi E, et al. Usefulness of a mouse myelin basic protein promoter for gene therapy of malignant glioma: myelin basic protein promoter is strongly active in human malignant glioma cells. *Jpn J Cancer Res Gann*. 1997;88:678–86.
16. Lo H-W. Targeting Ras-RAF-ERK and its interactive pathways as a novel therapy for malignant gliomas. *Curr Cancer Drug Targets*. 2010;10:840–8.

17. Badiali M, Gleize V, Paris S, Moi L, Elhouadani S, Arcella A, et al. KIAA1549-BRAF fusions and IDH mutations can coexist in diffuse gliomas of adults. *Brain Pathol Zurich Switz.* 2012;22:841–7.
18. Sonoki T, Harder L, Horsman DE, Karran L, Taniguchi I, Willis TG, et al. Cyclin D3 is a target gene of t(6;14)(p21.1;q32.3) of mature B-cell malignancies. *Blood.* 2001;98:2837–44.
19. Wlodarska I, Dierickx D, Vanhentenrijk V, Van Roosbroeck K, Pospisilova H, Minnei F, et al. Translocations targeting CCND2, CCND3, and MYCN do occur in t(11;14)-negative mantle cell lymphomas. *Blood.* 2008;111:5683–90.
20. Filipits M, Jaeger U, Pohl G, Stranzl T, Simonitsch I, Kaider A, et al. Cyclin D3 is a predictive and prognostic factor in diffuse large B-cell lymphoma. *Clin Cancer Res Off J Am Assoc Cancer Res.* 2002;8:729–33.

Table 1

Canine tumors	Gene 1	Gene 2	Chromosomal positions	Number of reads spanning the fusion junction	Number of paired reads encompassing the two fusion transcripts
Dermatofibrosarcoma protuberans-like (DFSP-like)	<i>PDGFB</i>	<i>COL3A1</i>	CFA10: 25,807,321 (strand -) / CFA36: 30,511,682 (strand -)	181	491
Anaplastic oligodendroglioma	<i>MBP</i>	<i>BRAF</i>	CFA1: 2,919,660 (strand +) / CFA16: 8,270,092 (strand +) CFA1: 2,923,624 (strand +) / CFA16: 8,264,593 (strand +) CFA16: 8,262,734 (strand +) / CFA1: 2,926,747 (strand +) CFA16: 8,270,092 (strand +) / CFA1: 2,919,740 (strand +)	115	344
Diffuse Large B-Cell Lymphoma (DLBCL)	<i>CCND3</i>	<i>IGK</i>	CFA12: 10,687,874 (strand -) / CFA17: 37,727,274 (strand +) CFA12: 10,687,876 (strand -) / CFA17: 37,709,802 (strand +)	15	10


Table 1: Fusions identified by RNA-Seq in the canine tumors. Partner genes and chromosomal positions are indicated for the three tumors with the number of reads spanning the fusion junction and encompassing the two fusion transcripts. CFA: *Canis familiaris* Autosome.

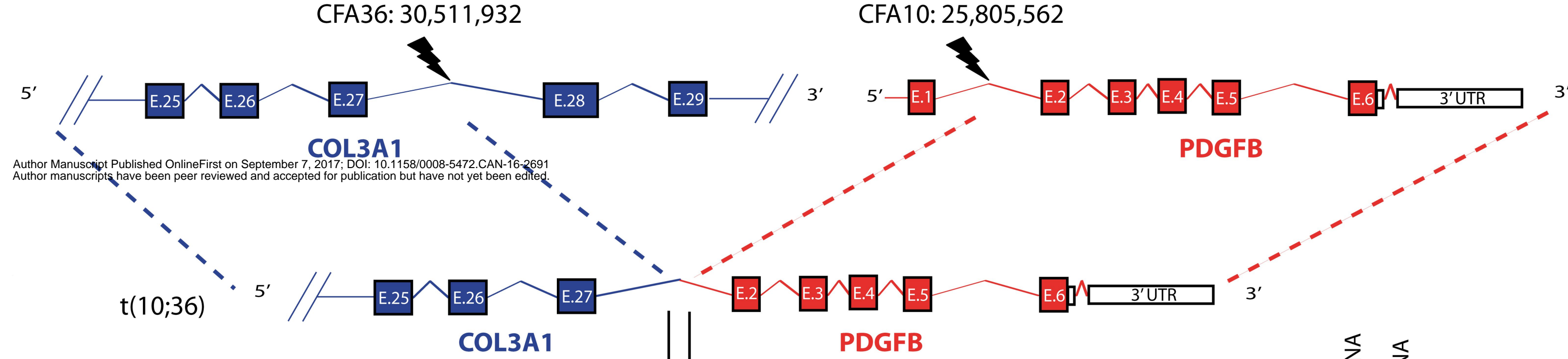
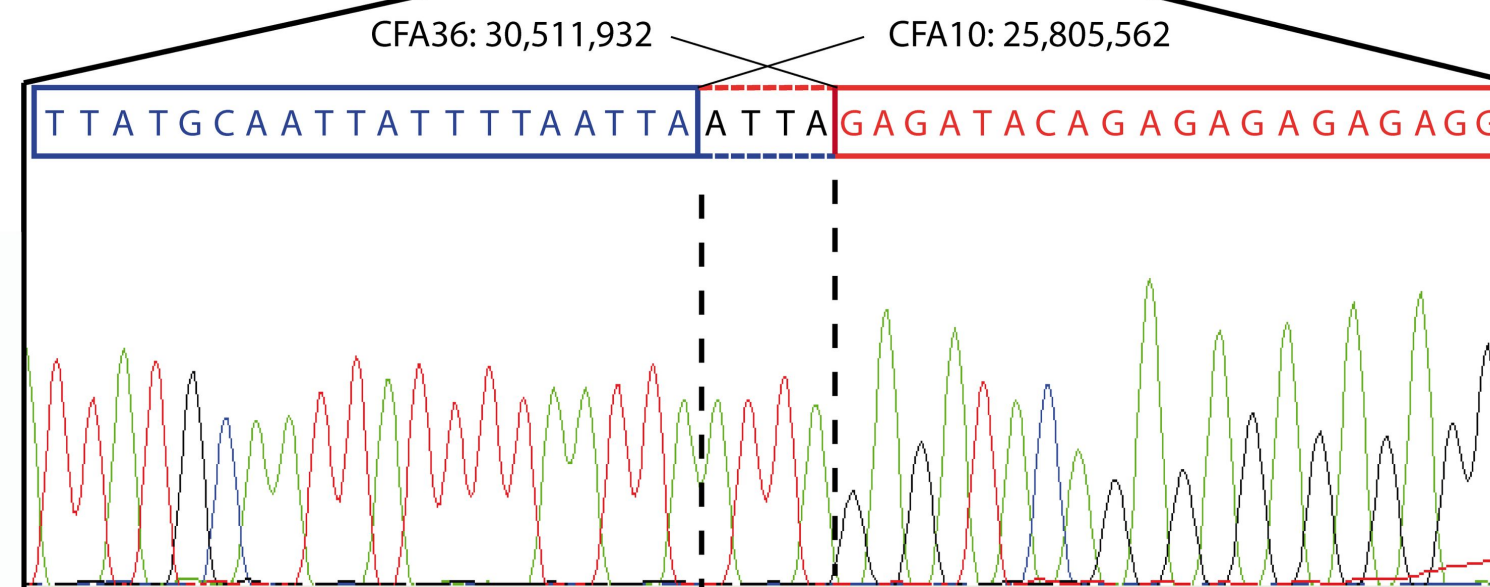
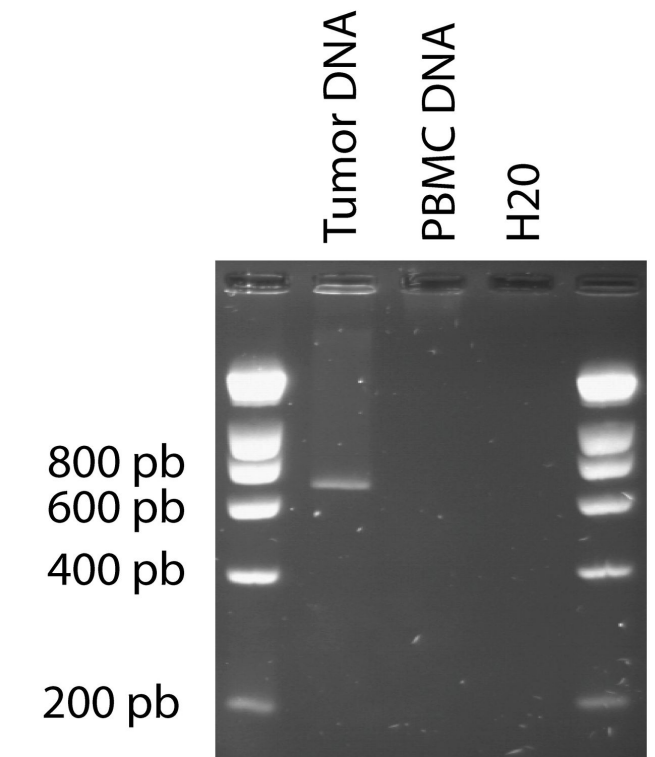
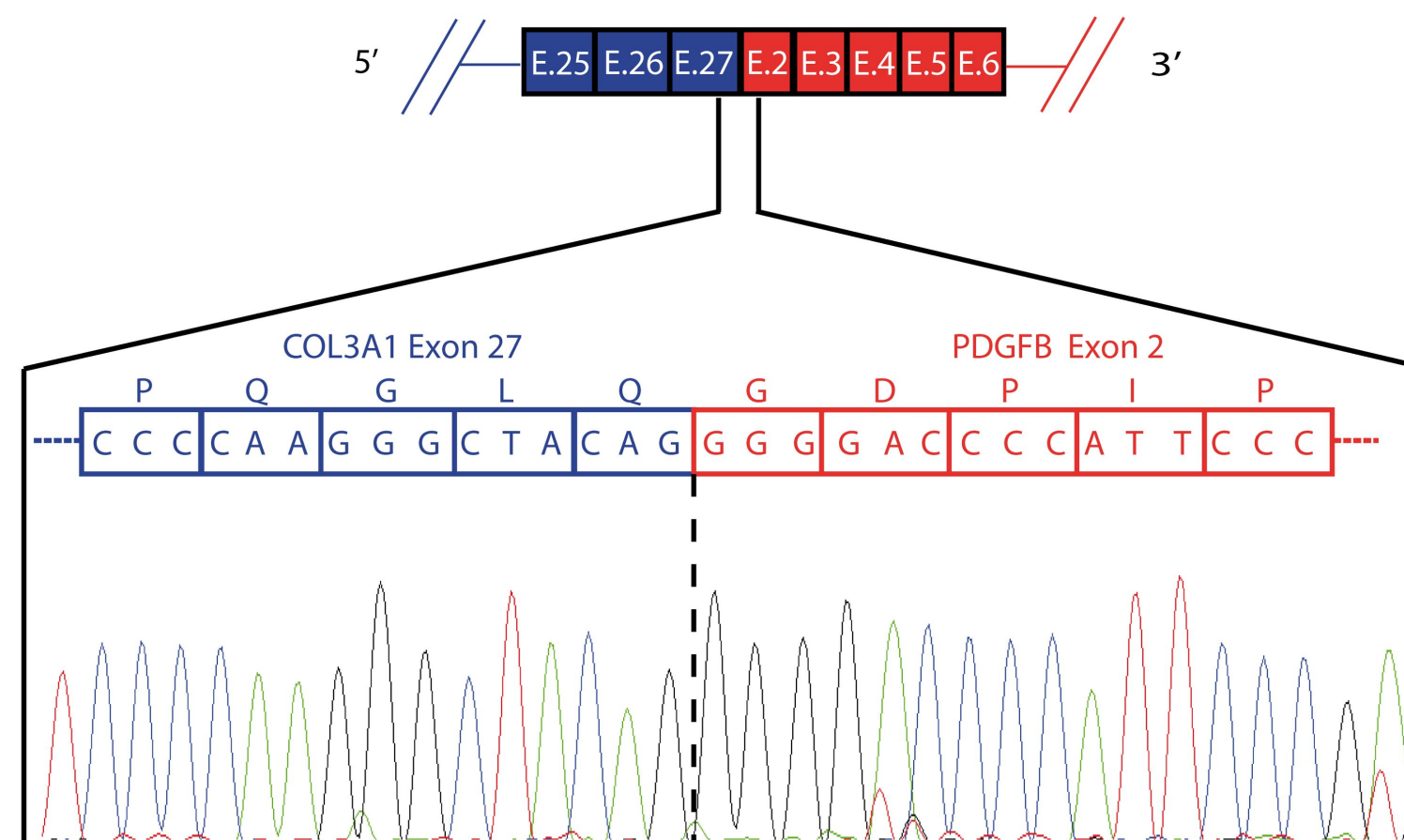
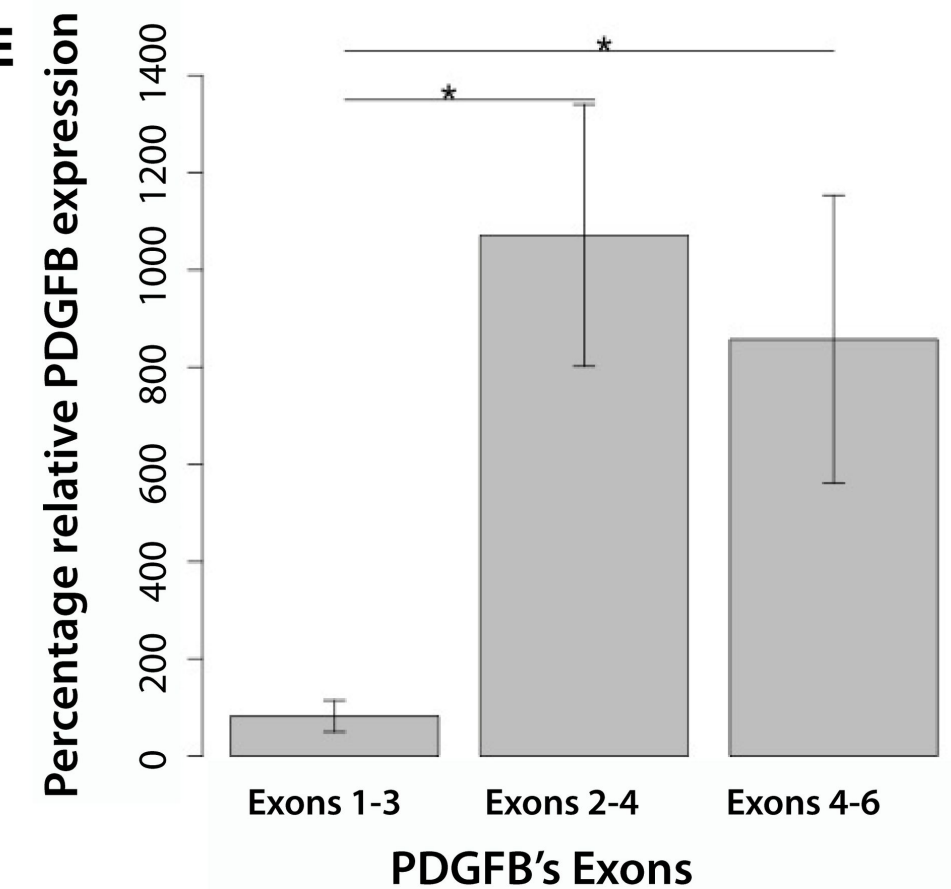
Figures Legends

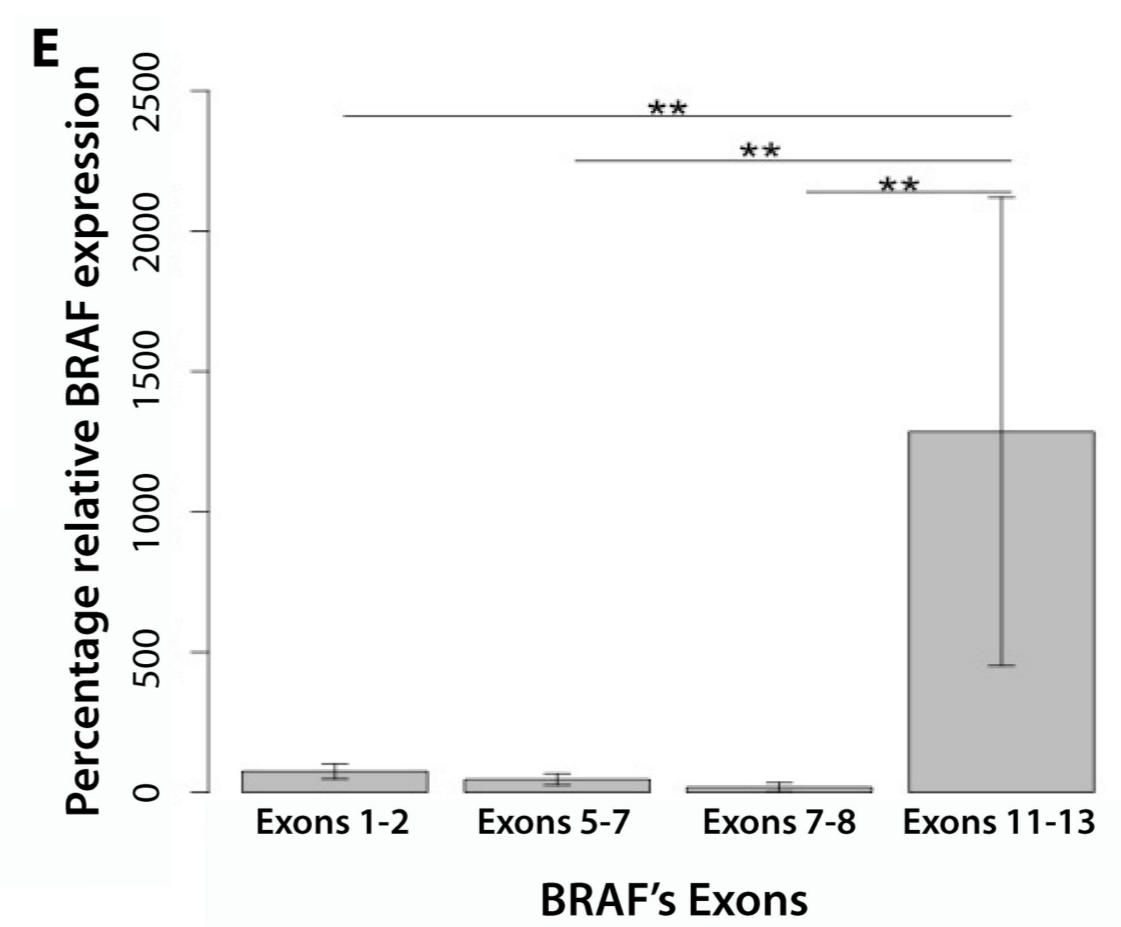
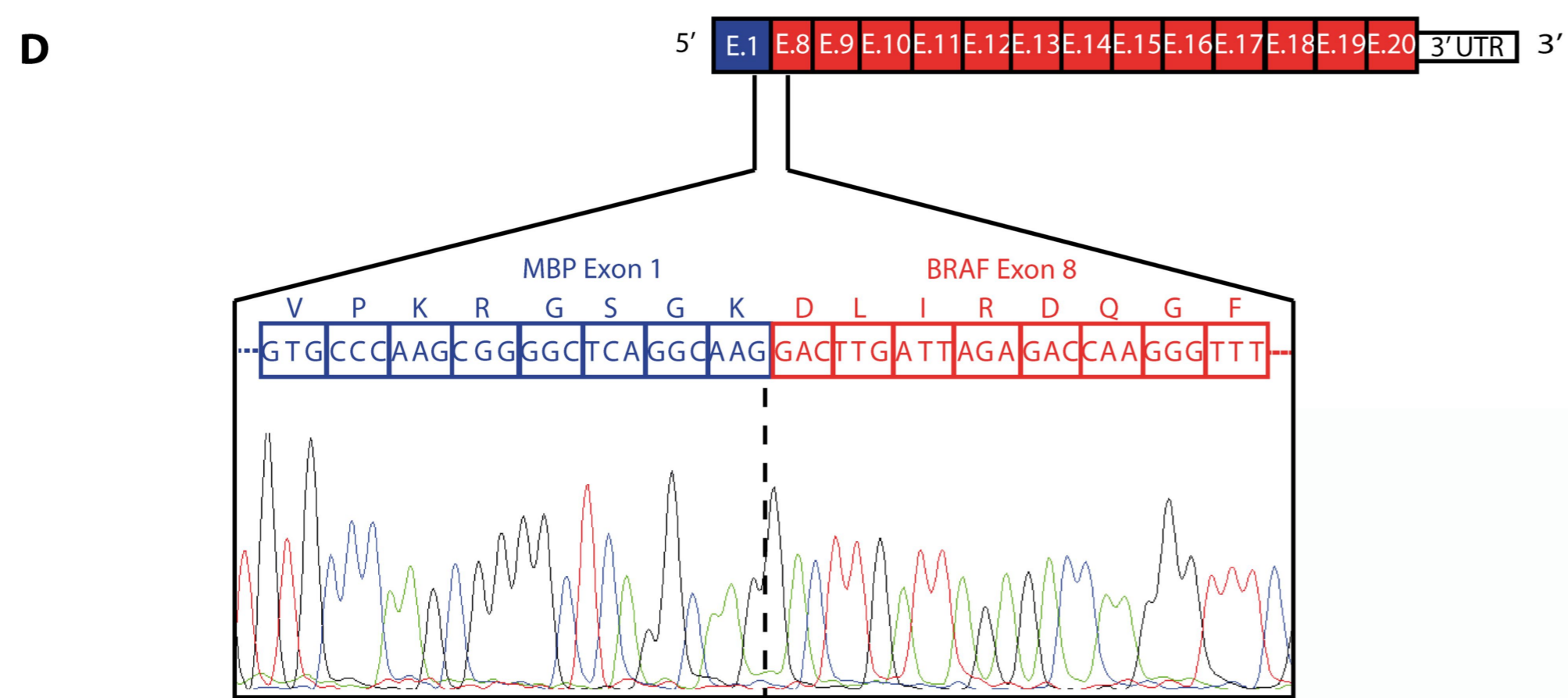
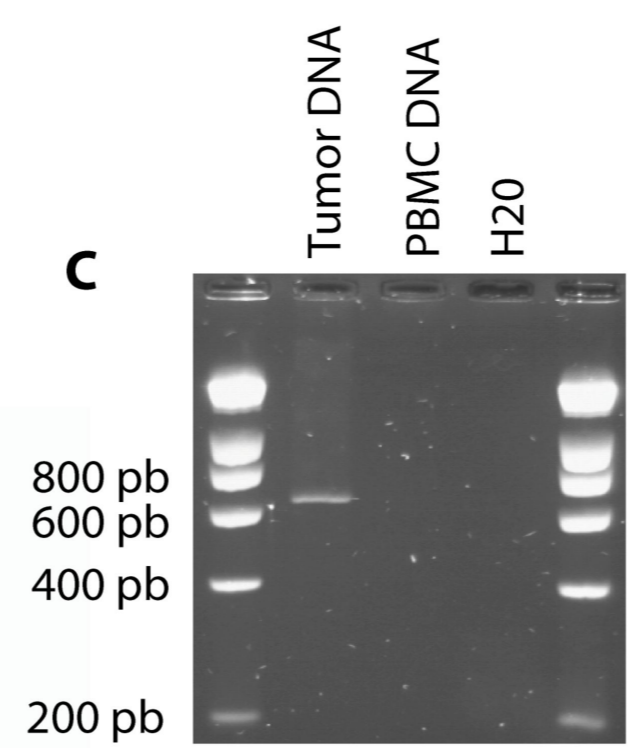
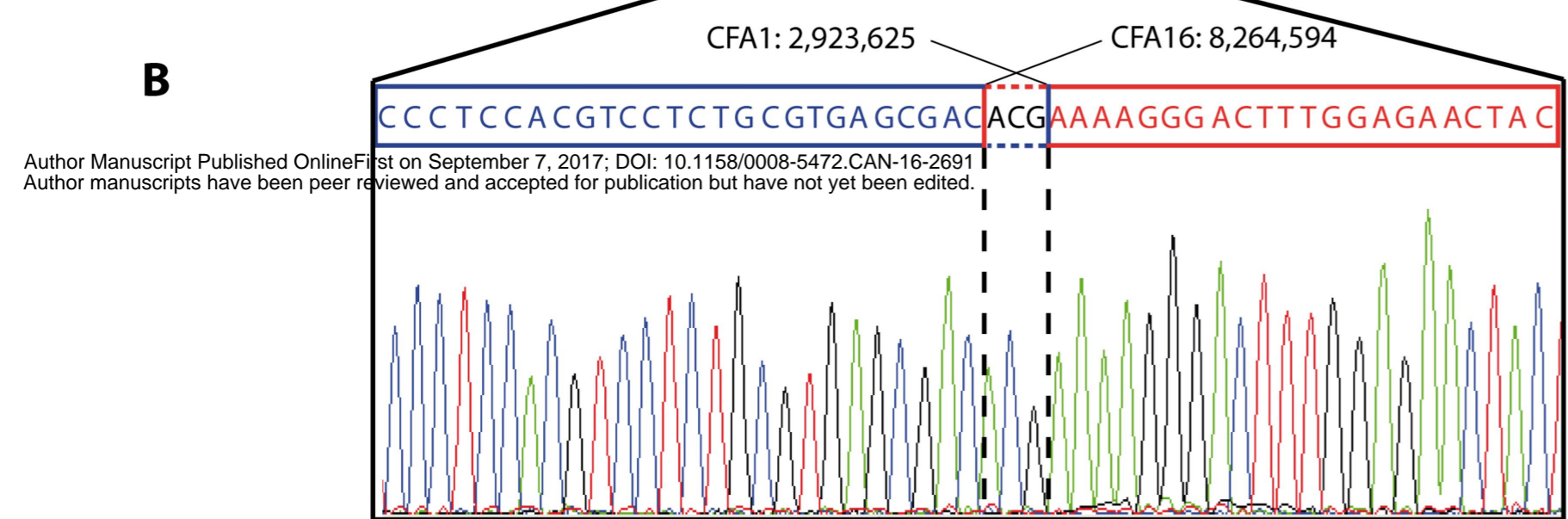
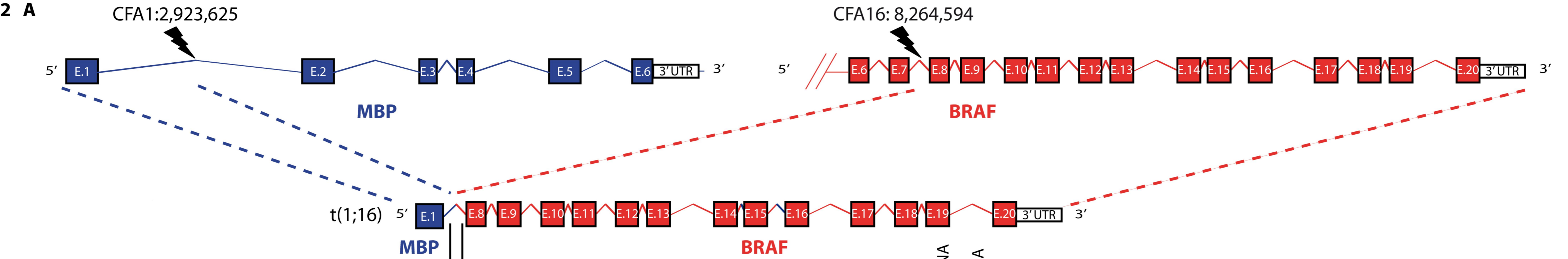
Figure 1: Characterization of the *COL3A1-PDGFB* fusion. (A) Scheme of the t(10;36). Exons of *COL3A1* (ENSCAFT00000047312) and *PDGFB* (ENSCAFT00000002101) are depicted as well as the breakpoint positions on CFA36 (blue) and CFA10 (red), indicated with ✂. CFA: *Canis familiaris* Autosome. (B) Sequence of the breakpoint on genomic DNA. The 3 nucleotides flanking the dotted line map to both chromosomes. (C) Electrophoresis of PCR products detects the translocation in tumor but not in the germinal blood DNA of this case. (D) Scheme of the transcription resulting from the t(10;36): the sequence of the tumor cDNA reveals the expression of one fusion transcript involving exon 27 of *COL3A1* and exon 2 of *PDGFB*. (E) Relative expression levels of *PDGFB* exons in the tumor in comparison with 6 healthy skin samples (* p-value < 0.05 one-tailed paired-samples Wilcoxon test). Expression levels of exons 2 to 6 show overexpression of *PDGFB* exons retained in the chimeric transcript. The *PDGFB* wild type transcript expression, represented by expression levels of exons 1-3, shows no significant difference in the tumor in comparison with an expected value of 100% (p-value = 0.31, two-tailed one sample Wilcoxon test). These results indicate that the overexpression of *PDGFB* exons in the chimeric transcript is the consequence of the fusion.

Figure 2: Characterization of the *MBP-BRAF* fusion. (A) Scheme of the t(1;16) translocation. Exons of *MBP* (ENSCAFT00000000024) and *BRAF* (ENSCAFT00000006305) are depicted as well the breakpoint positions on CFA1 (blue) and CFA16 (red) indicated with ✂. CFA: *Canis familiaris* Autosome. (B) Sequence of the breakpoint on genomic DNA. The 3 nucleotides flanking the dotted line map to both chromosomes. (C) Electrophoresis of the PCR product detecting the translocation in tumor DNA but not on germinal blood DNA of this case. (D) Scheme of the transcript resulting from the t(1;16) translocation: the sequence of the tumor cDNA reveals the expression of one fusion transcript involving the exon 1 of *MBP* with exon 8 of *BRAF*. (E) The histogram shows the relative expression levels of *BRAF* exons in the tumor in comparison with 8 healthy brain samples. The fusion induced overexpression of the retained exons 11-13 on average 12.8-fold (p-value ≤ 0.01, one-tailed Wilcoxon test) in comparison with healthy canine brain tissues. The retained exons are overexpressed in

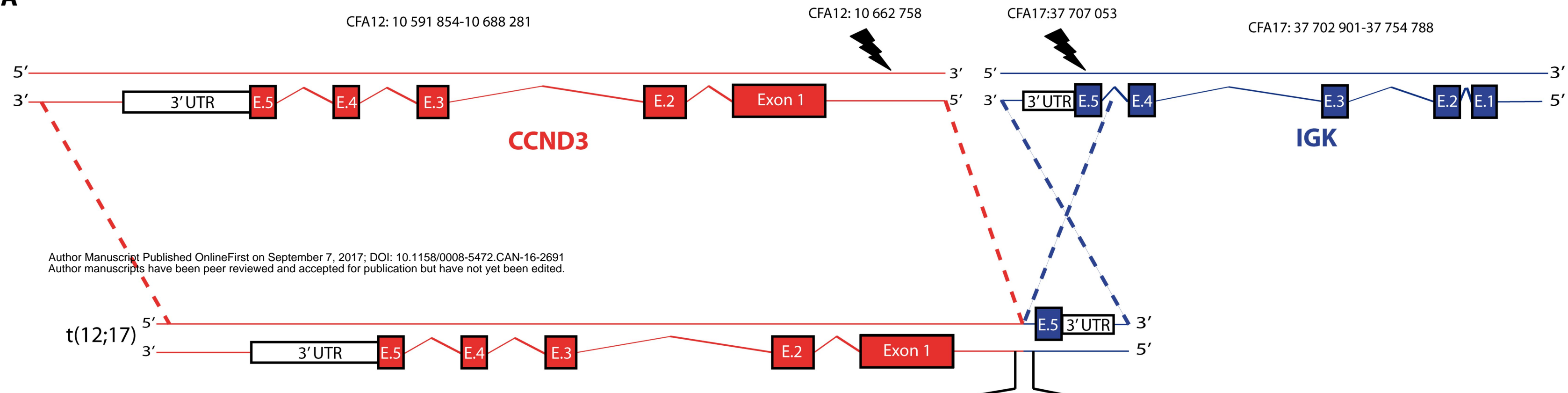
comparison to exons localized in 5' of the breakpoint (** p-value ≤ 0.01 , two-tailed paired two-Sample t-test). Expression levels of exons 7-8, flanking the breakpoint, showed that the *BRAF* wild type transcript is significantly under-expressed in the tumor (p-value ≤ 0.01 , one-tailed Wilcoxon test). These results showed that the overexpression of *BRAF* exons retained in the chimeric transcript is linked to the fusion.

Figure 3: Characterization of the *IGK-CCND3* translocation in a canine DLBCL. (A) Schematic representation of the t(12;17) translocation. Exons of *CCND3* (ENSCAFT0000002538) and *IGK* (ENSCAFT00000011790) are depicted as well as the breakpoint positions on CFA12 (red) and CFA17 (blue), indicated with . CFA: *Canis familiaris* Autosome. (B) Sequence of the breakpoint on genomic DNA. (C) Electrophoresis of the PCR product detecting the translocation in the tumor DNA but not in the germinal blood DNA of this case. (D) Scheme of the transcription resulting from t(12;17) translocation: the sequence of the tumor cDNA reveals the expression of one fusion transcript involving a not yet annotated exon of CFA12 with exon 5 of *IGK*. (E) RT-qPCR experiments show the overexpression of the *CCND3* mRNA transcript in the tumor, on average 13-fold (p-value < 0.05 one-tailed One-Sample Wilcoxon test) and 22-fold (**** p-value $< 10^{-4}$ one-tailed Two-Samples Wilcoxon test), as compared with 6 healthy lymph nodes and 6 other DLBCLs respectively.

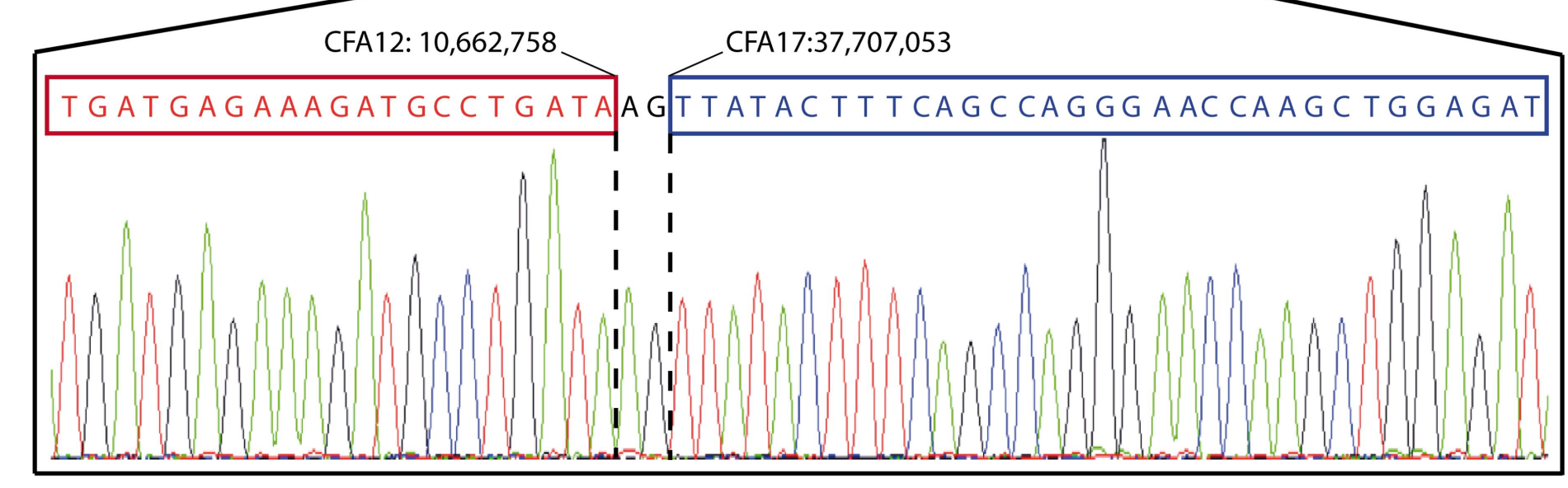
A**B****C****D****E**



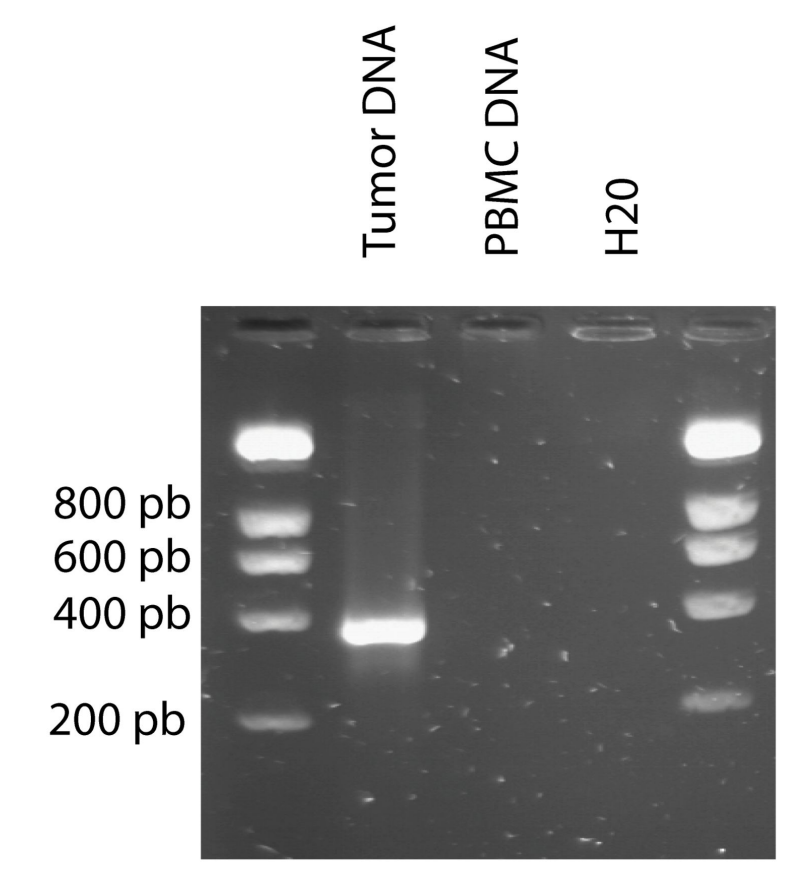
A



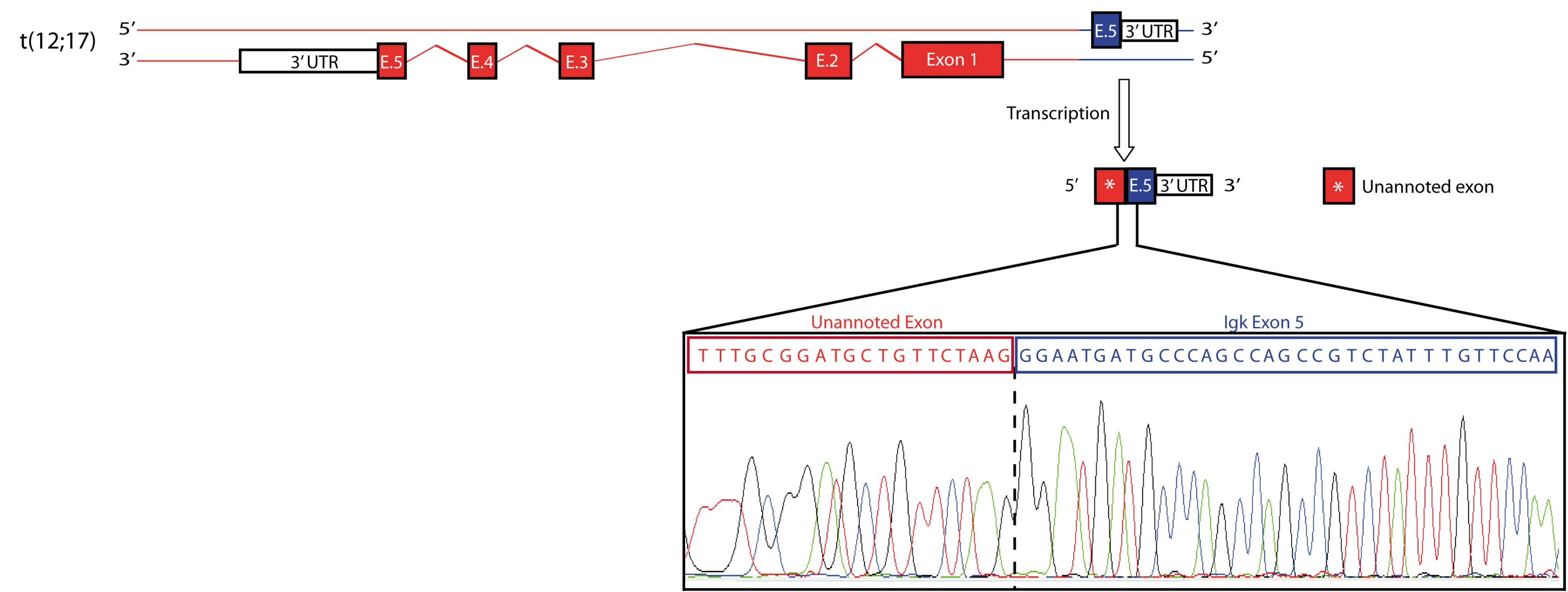
B



C



D



E

